

Photon emission in neutral current interactions at the MiniBooNE and T2K experiments

En Wang

Zhengzhou University

July 24, 2015

Overview

- 1 Introduction
- 2 Theoretical Model of $\text{NC}\gamma$
 - $\text{NC}\gamma$ on nucleon
 - Incoherent $\text{NC}\gamma$ on nuclei
 - Coherent $\text{NC}\gamma$ on nuclei
- 3 $\text{NC}\gamma$ events at MiniBooNE
- 4 $\text{NC}\gamma$ events at T2K

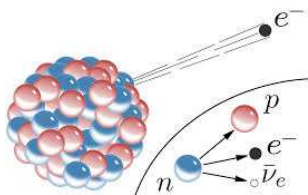
Introduction

Neutrino History

- In 1930, Wolfgang Pauli postulated an undetected particle 'neutron'. In 1933, Enrico Fermi developed the theory of beta decay and coined the term 'neutrino'.

Neutrino History

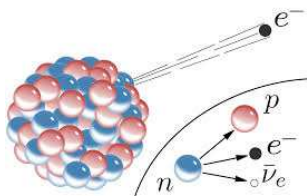
- In 1930, Wolfgang Pauli postulated an undetected particle 'neutron'. In 1933, Enrico Fermi developed the theory of beta decay and coined the term 'neutrino'.



- In order to explain how beta decay could conserve energy, momentum, and angular momentum (spin).

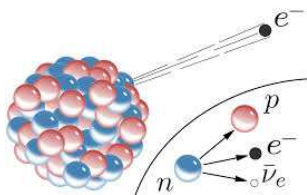
Neutrino History

- In 1930, Wolfgang Pauli postulated an undetected particle 'neutron'. In 1933, Enrico Fermi developed the theory of beta decay and coined the term 'neutrino'.
- In 1956, electron neutrino was detected in the Cowan-Reines neutrino experiment.
- In 1962, muon neutrino was discovered by Leon Lederman, Melvin Schwartz and Jack Steinberger. (Brookhaven AGS neutrino experiment)
- In 2000, the tau neutrino was detected by the DONUT collaboration at Fermilab.



Neutrino History

- In 1930, Wolfgang Pauli postulated an undetected particle 'neutron'. In 1933, Enrico Fermi developed the theory of beta decay and coined the term 'neutrino'.
- In 1956, electron neutrino was detected in the Cowan-Reines neutrino experiment.
- In 1962, muon neutrino was discovered by Leon Lederman, Melvin Schwartz and Jack Steinberger. (Brookhaven AGS neutrino experiment)
- In 2000, the tau neutrino was detected by the DONUT collaboration at Fermilab.



Standard Model

- Three flavor (at least): ν_e , ν_μ and ν_τ
- Chargeless, massless
- 1/2 spin

Neutrino Oscillation

- Recently, it has been observed that neutrinos can change their flavor and have non-zero masses, which is contrast to the prediction of the Standard Model of particle physics.

Neutrino Oscillation

- Recently, it has been observed that neutrinos can change their flavor and have non-zero masses, which is contrast to the prediction of the Standard Model of particle physics.
- To address these questions, several experiments have been designed for obtaining a precise determination of the mass-squared differences and the flavor-mixing angles.

Neutrino Oscillation

- Recently, it has been observed that neutrinos can change their flavor and have non-zero masses, which is contrast to the prediction of the Standard Model of particle physics.
- To address these questions, several experiments have been designed for obtaining a precise determination of the mass-squared differences and the flavor-mixing angles.
- As we know, neutrinos only interact with matter through weak interactions, and the cross sections are tiny, so it is very challenging to detect the neutrino.

Neutrino Oscillation

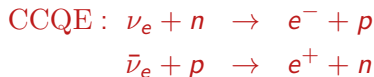
- Recently, it has been observed that neutrinos can change their flavor and have non-zero masses, which is contrast to the prediction of the Standard Model of particle physics.
- To address these questions, several experiments have been designed for obtaining a precise determination of the mass-squared differences and the flavor-mixing angles.
- As we know, neutrinos only interact with matter through weak interactions, and the cross sections are tiny, so it is very challenging to detect the neutrino.
- Neutrino-nucleus interactions in the medium-energy region (~ 1 GeV), which length is hadronic (~ 1 fm), are strongly modified by nuclear effects.

Neutrino Oscillation

- Recently, it has been observed that neutrinos can change their flavor and have non-zero masses, which is contrast to the prediction of the Standard Model of particle physics.
- To address these questions, several experiments have been designed for obtaining a precise determination of the mass-squared differences and the flavor-mixing angles.
- As we know, neutrinos only interact with matter through weak interactions, and the cross sections are tiny, so it is very challenging to detect the neutrino.
- Neutrino-nucleus interactions in the medium-energy region (~ 1 GeV), which length is hadronic (~ 1 fm), are strongly modified by nuclear effects.
- A good understanding of (anti)neutrino cross sections is crucial to reduce the systematic uncertainties in oscillation experiments aiming at a precise determination of neutrino properties.

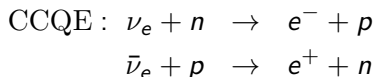
Neutral Current photon emission

- One of the possible reaction channels is photon emission induced by neutral current (NC) interactions (NC γ), which turns out to be one of the largest backgrounds in $\nu_\mu \rightarrow \nu_e$ ($\bar{\nu}_\mu \rightarrow \bar{\nu}_e$) oscillation experiments where electromagnetic showers produced by electrons (positrons) and photons are not distinguishable.



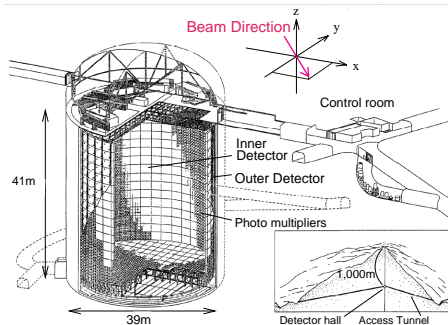
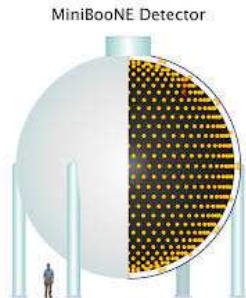
Neutral Current photon emission

- One of the possible reaction channels is photon emission induced by neutral current (NC) interactions (NC γ), which turns out to be one of the largest backgrounds in $\nu_\mu \rightarrow \nu_e$ ($\bar{\nu}_\mu \rightarrow \bar{\nu}_e$) oscillation experiments where electromagnetic showers produced by electrons (positrons) and photons are not distinguishable.

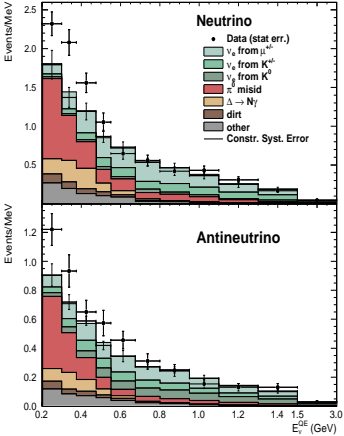


- The detector of MiniBooNE, and the far detector (Super-Kamiokande, SK) of the T2K experiment, are water Cherenkov detector. They are incapable of discriminating the diffuse rings of e^\pm originated in charged current interactions by electron neutrinos from those created by photons.

The detectors of MiniBooNE and SK



Electron-like Events at MiniBooNE

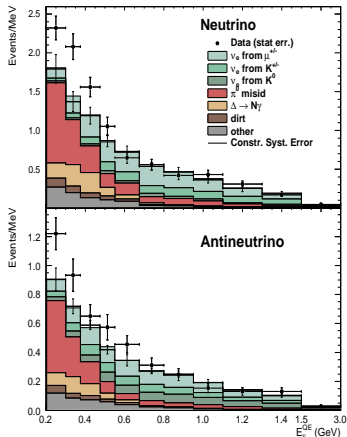


Electron-like Events at MiniBooNE

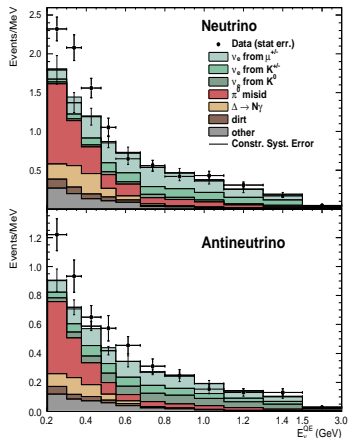
- excess events over predicted backgrounds

A. Aguilar-Arevalo et al., PRL 110(2013),161801

- ▶ ν -mode excess: 162.0 ± 47.8 events
- ▶ $\bar{\nu}$ -mode excess: 78.4 ± 28.5 events



Electron-like Events at MiniBooNE

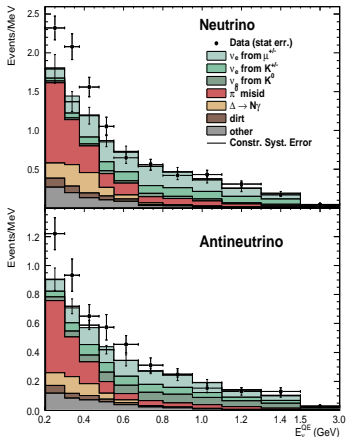


- excess events over predicted backgrounds

A. Aguilar-Arevalo et al., PRL 110(2013),161801

- ▶ ν -mode excess: 162.0 ± 47.8 events
- ▶ $\bar{\nu}$ -mode excess: 78.4 ± 28.5 events
- In the $\bar{\nu}$ mode, the data are found to be consistent with $\bar{\nu}_\mu \rightarrow \bar{\nu}_e$ oscillations.
- In the ν mode, the data show a clear (3σ) excess of signal-like events at low reconstructed neutrino energies ($200 < E_\nu^{QE} < 475$ MeV).

Electron-like Events at MiniBooNE



- This anomaly can't be explained by the existence of 1, 2, or 3 families of sterile neutrinos.

J. Conrad, et al., AHEP 2013(2013), 163897;

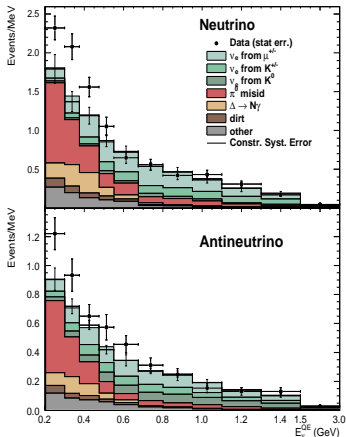
C. Giunti, et al., PRD 88(2013), 073008.

- Lorentz violation T. Katori, PRD 74(2006), 105009.

- Radiative decay of heavy neutrinos

S. Gninenko, PRL 103(2009), 241802.

Electron-like Events at MiniBooNE



- This anomaly can't be explained by the existence of 1, 2, or 3 families of sterile neutrinos.

J. Conrad, et al., AHEP 2013(2013), 163897;

C. Giunti, et al., PRD 88(2013), 073008.

- Lorentz violation T. Katori, PRD 74(2006), 105009.

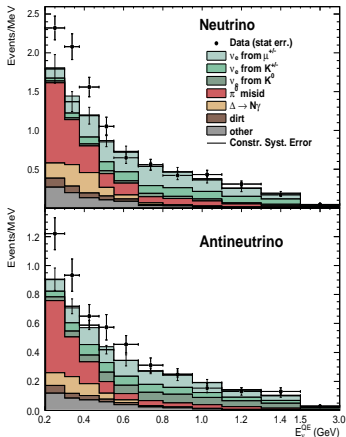
- Radiative decay of heavy neutrinos

S. Gninenko, PRL 103(2009), 241802.

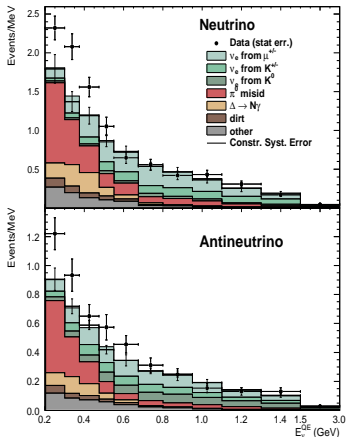
- It could have its origin in poorly understood background and unknown systematics.

Electron-like Events at MiniBooNE

- $\text{NC}\pi^0$ where the $\gamma\gamma$ decay is not identified
This background has been constrained by MiniBooNE's $\text{NC}\pi^0$ measurement.

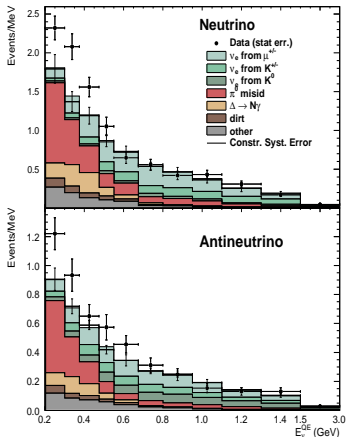


Electron-like Events at MiniBooNE



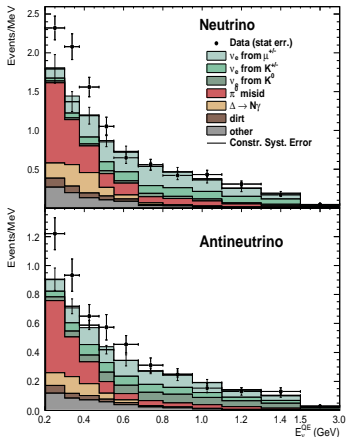
- $\text{NC}\pi^0$ where the $\gamma\gamma$ decay is not identified
This background has been constrained by MiniBooNE's $\text{NC}\pi^0$ measurement.
- $\text{NC}\gamma$ — the second largest background
The MiniBooNE analysis estimated this background using the $\text{NC}\pi^0$ measurement, assuming that $\text{NC}\gamma$ events come from the radiative decay of weakly produced resonances, mainly $\Delta \rightarrow N\gamma$.

Electron-like Events at MiniBooNE



- $\text{NC}\pi^0$ where the $\gamma\gamma$ decay is not identified
This background has been constrained by MiniBooNE's $\text{NC}\pi^0$ measurement.
- $\text{NC}\gamma$ — the second largest background
The MiniBooNE analysis estimated this background using the $\text{NC}\pi^0$ measurement, assuming that $\text{NC}\gamma$ events come from the radiative decay of weakly produced resonances, mainly $\Delta \rightarrow N\gamma$.
- If the $\text{NC}\gamma$ emission estimate were not sufficiently accurate, this would be relevant to track the origin of the observed excess.

Electron-like Events at MiniBooNE



- $\text{NC}\pi^0$ where the $\gamma\gamma$ decay is not identified
This background has been constrained by MiniBooNE's $\text{NC}\pi^0$ measurement.
- $\text{NC}\gamma$ — the second largest background
The MiniBooNE analysis estimated this background using the $\text{NC}\pi^0$ measurement, assuming that $\text{NC}\gamma$ events come from the radiative decay of weakly produced resonances, mainly $\Delta \rightarrow N\gamma$.
- If the $\text{NC}\gamma$ emission estimate were not sufficiently accurate, this would be relevant to track the origin of the observed excess.
- It is therefore very important to have a robust theoretical understanding of the NC photon emission reaction, which cannot be unambiguously constrained by data.

Theoretical Model of $\text{NC}\gamma$

(PRC 89(2014),015503)

Reactions of Neutral Current Photon emission

NC γ on single nucleons:

$$\nu/\bar{\nu} + N \rightarrow \nu/\bar{\nu} + N + \gamma$$

and on nuclear targets:

$$\nu/\bar{\nu} + A \rightarrow \nu/\bar{\nu} + X + \gamma$$

$$\nu/\bar{\nu} + A \rightarrow \nu/\bar{\nu} + A + \gamma$$

Reactions of Neutral Current Photon emission

NC γ on single nucleons:

$$\nu/\bar{\nu} + N \rightarrow \nu/\bar{\nu} + N + \gamma$$

and on nuclear targets:

$$\nu/\bar{\nu} + A \rightarrow \nu/\bar{\nu} + X + \gamma$$

$$\nu/\bar{\nu} + A \rightarrow \nu/\bar{\nu} + A + \gamma$$

- At the relevant energies for MiniBooNE and T2K experiments (~ 1 GeV), the reaction is dominated by the excitation of the $\Delta(1232)$ resonance, but there are also non-resonant contributions that, close to threshold, are fully determined by the effective chiral Lagrangian of strong interactions.

Reactions of Neutral Current Photon emission

NC γ on single nucleons:

$$\nu/\bar{\nu} + N \rightarrow \nu/\bar{\nu} + N + \gamma$$

and on nuclear targets:

$$\nu/\bar{\nu} + A \rightarrow \nu/\bar{\nu} + X + \gamma$$

$$\nu/\bar{\nu} + A \rightarrow \nu/\bar{\nu} + A + \gamma$$

- At the relevant energies for MiniBooNE and T2K experiments (~ 1 GeV), the reaction is dominated by the excitation of the $\Delta(1232)$ resonance, but there are also non-resonant contributions that, close to threshold, are fully determined by the effective chiral Lagrangian of strong interactions.
- We have extended the model to nuclear targets taking into account nuclear effects.

Theoretical Model – $\text{NC}\gamma$ on nucleon

Amplitude for $NC\gamma$ on Nucleon

The differential cross section for the reactions

$$\begin{aligned}\nu_l(k) + N(p) &\rightarrow \nu_l(k') + N(p') + \gamma(k_\gamma), \\ \bar{\nu}_l(k) + N(p) &\rightarrow \bar{\nu}_l(k') + N(p') + \gamma(k_\gamma)\end{aligned}$$

is given by,

$$\frac{d^3\sigma_{(\nu,\bar{\nu})}}{dE_\gamma d\Omega(\hat{k}_\gamma)} = \frac{E_\gamma}{|\vec{k}|} \frac{G^2}{16\pi^2} \int \frac{d^3k'}{|\vec{k}'|} L_{\mu\sigma}^{(\nu,\bar{\nu})} W^{\mu\sigma},$$

The leptonic tensor

$$L_{\mu\sigma}^{(\nu,\bar{\nu})} = k'_\mu k_\sigma + k'_\sigma k_\mu + g_{\mu\sigma} \frac{q^2}{2} \pm i\epsilon_{\mu\sigma\alpha\beta} k'^\alpha k^\beta,$$

the hadronic one

$$W^{\mu\sigma} = \frac{1}{4m_N} \sum_{\text{spins}} \int \frac{d^3p'}{(2\pi)^3} \frac{1}{2E'_N} \delta^4(p' + k_\gamma - q - p) \langle N\gamma | j^\mu(0) | N \rangle \langle N\gamma | j^\sigma(0) | N \rangle^*,$$

The amputated amplitudes

In terms of the amputated amplitudes

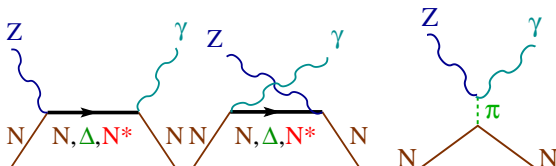
$$W^{\mu\sigma} = -\frac{1}{8m_N} \int \frac{d^3 p'}{(2\pi)^3} \frac{1}{2E'_N} \delta^4(p' + k_\gamma - q - p) \text{Tr} [(\not{p}' + m_N)\Gamma^{\mu\rho}(\not{p} + m_N)\gamma^0(\Gamma^\sigma_\rho)^\dagger\gamma^0],$$

with

$$\Gamma_N^{\mu\rho} = \sum_a \Gamma_a^{\mu\rho}, \quad a = BP, CBP, \pi Ex, \text{ and}$$

$$B = N, \Delta(1232), N(1440), N(1520), N(1535).$$

Explicit expressions for these amplitudes can be found in [Phys.Rev. C89 (2014), 015503].



Nucleon Pole Terms

$$\Gamma_N^{\mu\alpha} = \tilde{J}_{EM}^\mu(q_\gamma)(\not{p} + \not{q} + M)J_{NC}^\alpha(q)D_N(p+q) + \tilde{J}_{NC}^\alpha(-q)(\not{p}' - \not{q} + M)J_{EM}^\mu(-q_\gamma)D_N(p'-q)$$



Nucleon Pole Terms

$$\Gamma_N^{\mu\alpha} = \tilde{J}_{EM}^\mu(q_\gamma)(\not{p} + \not{q} + M)J_{NC}^\alpha(q)D_N(p+q) + \tilde{J}_{NC}^\alpha(-q)(\not{p}' - \not{q} + M)J_{EM}^\mu(-q_\gamma)D_N(p'-q)$$



$$J_{NC}^\alpha(q) = \gamma^\alpha \tilde{F}_1(q^2) + \frac{i}{2M} \sigma^{\alpha\beta} q_\beta \tilde{F}_2(q^2) - \gamma^\alpha \gamma_5 \tilde{F}_A(q^2),$$

$$J_{EM}^\mu(q_\gamma) = \gamma^\mu F_1(0) + \frac{i}{2M} \sigma^{\mu\nu} q_{\nu} F_2(0),$$

Nucleon Pole Terms

$$\Gamma_N^{\mu\alpha} = \tilde{J}_{EM}^\mu(q_\gamma)(\not{p} + \not{q} + M)J_{NC}^\alpha(q)D_N(p+q) + \tilde{J}_{NC}^\alpha(-q)(\not{p}' - \not{q} + M)J_{EM}^\mu(-q_\gamma)D_N(p' - q)$$



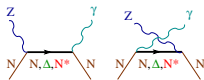
$$J_{NC}^\alpha(q) = \gamma^\alpha \tilde{F}_1(q^2) + \frac{i}{2M} \sigma^{\alpha\beta} q_\beta \tilde{F}_2(q^2) - \gamma^\alpha \gamma_5 \tilde{F}_A(q^2),$$

$$J_{EM}^\mu(q_\gamma) = \gamma^\mu F_1(0) + \frac{i}{2M} \sigma^{\mu\nu} q_{\nu} F_2(0),$$

$$D_N(p) = \frac{1}{\not{p} - M} \leftarrow \text{nucleon propagator}$$

Nucleon Pole Terms

$$\Gamma_N^{\mu\alpha} = \tilde{J}_{EM}^\mu(q_\gamma)(\not{p} + \not{q} + M)J_{NC}^\alpha(q)D_N(p+q) + \tilde{J}_{NC}^\alpha(-q)(\not{p}' - \not{q} + M)J_{EM}^\mu(-q_\gamma)D_N(p'-q)$$



$$J_{NC}^\alpha(q) = \gamma^\alpha \tilde{F}_1(q^2) + \frac{i}{2M} \sigma^{\alpha\beta} q_\beta \tilde{F}_2(q^2) - \gamma^\alpha \gamma_5 \tilde{F}_A(q^2),$$

$$J_{EM}^\mu(q_\gamma) = \gamma^\mu F_1(0) + \frac{i}{2M} \sigma^{\mu\nu} q_{\nu} F_2(0),$$

The NC vector form factors can be related to the EM ones by the isospin symmetry relationships,

$$\tilde{F}_{1,2}^{(p)} = (1 - 4 \sin^2 \theta_W) F_{1,2}^{(p)} - F_{1,2}^{(n)} - F_{1,2}^{(s)}$$

$$\tilde{F}_{1,2}^{(n)} = (1 - 4 \sin^2 \theta_W) F_{1,2}^{(n)} - F_{1,2}^{(p)} - F_{1,2}^{(s)}$$

$$F_{1,2}^{(s)} \leftarrow \text{to be neglected}$$

Nucleon Pole Terms

$$\Gamma_N^{\mu\alpha} = \tilde{J}_{EM}^\mu(q_\gamma)(\not{p} + \not{q} + M)J_{NC}^\alpha(q)D_N(p+q) + \tilde{J}_{NC}^\alpha(-q)(\not{p}' - \not{q} + M)J_{EM}^\mu(-q_\gamma)D_N(p'-q)$$



$$J_{NC}^\alpha(q) = \gamma^\alpha \tilde{F}_1(q^2) + \frac{i}{2M} \sigma^{\alpha\beta} q_\beta \tilde{F}_2(q^2) - \gamma^\alpha \gamma_5 \tilde{F}_A(q^2),$$

$$J_{EM}^\mu(q_\gamma) = \gamma^\mu F_1(0) + \frac{i}{2M} \sigma^{\mu\nu} q_{\nu} F_2(0),$$

$$\tilde{F}_A^{(p,n)} = \pm F_A - F_A^{(s)}, \quad (+ \rightarrow p, - \rightarrow n)$$

$$F_A(q^2) = g_A \left(1 - \frac{q^2}{M_A^2}\right)^{-2}$$

$$g_A = 1.267, \quad M_A = 1.016 \text{ GeV}$$

$$F_A^{(s)} \leftarrow \text{to be neglected}$$

$\Delta(1232)$ Pole Terms

$$\Gamma^{\mu\alpha} = \tilde{J}_{EM}^{\delta\mu}(p', q_\gamma) \Lambda_{\delta\sigma}(p+q) J_{NC}^{\sigma\alpha}(p, q) D_\Delta(p+q),$$

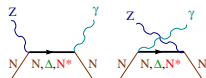
$$+ \tilde{J}_{NC}^{\delta\alpha}(p', -q) \Lambda_{\delta\sigma}(p'-q) J_{EM}^{\sigma\mu}(p, -q_\gamma) D_\Delta(p'-q),$$



$\Delta(1232)$ Pole Terms

$$\Gamma^{\mu\alpha} = \tilde{J}_{EM}^{\delta\mu}(p', q_\gamma) \Lambda_{\delta\sigma}(p+q) J_{NC}^{\sigma\alpha}(p, q) D_\Delta(p+q),$$

$$+ \tilde{J}_{NC}^{\delta\alpha}(p', -q) \Lambda_{\delta\sigma}(p'-q) J_{EM}^{\sigma\mu}(p, -q_\gamma) D_\Delta(p'-q),$$



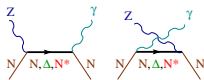
- Δ propagator,

$$D_\Delta(p) = \frac{1}{p^2 - M_\Delta^2 + iM_\Delta\Gamma_\Delta(p^2)}$$

$\Delta(1232)$ Pole Terms

$$\Gamma^{\mu\alpha} = \tilde{J}_{EM}^{\delta\mu}(p', q_\gamma) \Lambda_{\delta\sigma}(p+q) J_{NC}^{\sigma\alpha}(p, q) D_\Delta(p+q),$$

$$+ \tilde{J}_{NC}^{\delta\alpha}(p', -q) \Lambda_{\delta\sigma}(p'-q) J_{EM}^{\sigma\mu}(p, -q_\gamma) D_\Delta(p'-q),$$



- Δ propagator,


$$D_\Delta(p) = \frac{1}{p^2 - M_\Delta^2 + iM_\Delta\Gamma_\Delta(p^2)}$$

- The spin 3/2 projection operator,

$$\Lambda^{\mu\nu}(p_\Delta) = -(p_\Delta + M_\Delta) \left[g^{\mu\nu} - \frac{1}{3} \gamma^\mu \gamma^\nu - \frac{2}{3} \frac{p_\Delta^\mu p_\Delta^\nu}{M_\Delta^2} + \frac{1}{3} \frac{p_\Delta^\mu \gamma^\nu - p_\Delta^\nu \gamma^\mu}{M_\Delta} \right].$$

$\Delta(1232)$ Pole Terms

$$\Gamma^{\mu\alpha} = \tilde{J}_{EM}^{\delta\mu}(p', q_\gamma) \Lambda_{\delta\sigma}(p+q) J_{NC}^{\sigma\alpha}(p, q) D_\Delta(p+q),$$

$$+ \tilde{J}_{NC}^{\delta\alpha}(p', -q) \Lambda_{\delta\sigma}(p'-q) J_{EM}^{\sigma\mu}(p, -q_\gamma) D_\Delta(p'-q),$$


$$J_{NC}^{\beta\mu}(p, q) = \left[\frac{\tilde{C}_3^V(q^2)}{M} (g^{\beta\mu} \not{q} - q^\beta \gamma^\mu) + \frac{\tilde{C}_4^V(q^2)}{M^2} (g^{\beta\mu} q \cdot p_\Delta - q^\beta p_\Delta^\mu) \right. \\ \left. + \frac{\tilde{C}_5^V(q^2)}{M^2} (g^{\beta\mu} q \cdot p - q^\beta p^\mu) \right] \gamma_5 + \frac{\tilde{C}_3^A(q^2)}{M} (g^{\beta\mu} \not{q} - q^\beta \gamma^\mu) \\ + \frac{\tilde{C}_4^A(q^2)}{M^2} (g^{\beta\mu} q \cdot p_\Delta - q^\beta p_\Delta^\mu) + \frac{\tilde{C}_5^A(q^2)}{M^2} g^{\beta\mu},$$

$$J_{EM}^{\beta\mu}(p, -q_\gamma) = - \left[\frac{C_3^V(0)}{M} (g^{\beta\mu} \not{q}_\gamma - q_\gamma^\beta \gamma^\mu) + \frac{C_4^V(0)}{M^2} (g^{\beta\mu} q_\gamma \cdot p_{\Delta c} - q_\gamma^\beta p_{\Delta c}^\mu) \right. \\ \left. + \frac{C_5^V(0)}{M^2} (g^{\beta\mu} q_\gamma \cdot p - q_\gamma^\beta p^\mu) \right] \gamma_5,$$

$\Delta(1232)$ Pole Terms – Form Factors

- \tilde{C}_i^V — NC vector form factors
- C_i^V — EM transition form factors

$\Delta(1232)$ Pole Terms – Form Factors

- \tilde{C}_i^V — NC vector form factors
- C_i^V — EM transition form factors

The NC vector form factors are related to the EM ones

$$\tilde{C}_i^V(q^2) = (1 - 2 \sin^2 \theta_W) C_i^V(q^2)$$

$\Delta(1232)$ Pole Terms – Form Factors

- \tilde{C}_i^V — NC vector form factors
- C_i^V — EM transition form factors

The NC vector form factors are related to the EM ones

$$\tilde{C}_i^V(q^2) = (1 - 2 \sin^2 \theta_W) C_i^V(q^2)$$

$N - \Delta$ EM form factors C_i^V can be obtained from the helicity amplitudes, $A_{1/2}$, $A_{3/2}$ and $S_{1/2}$.

$\Delta(1232)$ Pole Terms – Form Factors

- \tilde{C}_i^V — NC vector form factors
- C_i^V — EM transition form factors

The helicity amplitudes, $A_{1/2}$, $A_{3/2}$ and $S_{1/2}$, are extracted from **pion photo- and electro-production**.

$$\mathcal{A}_{1/2} = \sqrt{\frac{2\pi\alpha}{k_R}} \left\langle S_z^* = \frac{1}{2} \left| \epsilon_\mu^{(+)} J_{EM}^\mu \right| S_z = -\frac{1}{2} \right\rangle \frac{1}{\sqrt{2M}\sqrt{2M_R}},$$

$$\mathcal{A}_{3/2} = \sqrt{\frac{2\pi\alpha}{k_R}} \left\langle S_z^* = \frac{3}{2} \left| \epsilon_\mu^{(+)} J_{EM}^\mu \right| S_z = \frac{1}{2} \right\rangle \frac{1}{\sqrt{2M}\sqrt{2M_R}},$$

$$\mathcal{S}_{1/2} = -\sqrt{\frac{2\pi\alpha}{k_R}} \left\langle S_z^* = \frac{1}{2} \left| \frac{|\vec{k}|}{\sqrt{Q^2}} \epsilon_\mu^{(0)} J_{EM}^\mu \right| S_z = \frac{1}{2} \right\rangle \frac{1}{\sqrt{2M}\sqrt{2M_R}},$$

We adopt the parametrization of the helicity amplitudes obtained in the **MAID** analysis.

D. Drechsel, et al., EPJA 34(2007),69 and <http://www.kph.uni-mainz.de/MAID>

$\Delta(1232)$ Pole Terms – Form Factors

- \tilde{C}_i^V — NC vector form factors
- C_i^V — EM transition form factors
- \tilde{C}_i^A — NC axial form factors

We assume a **standard dipole form** for the axial NC form factors

$$\tilde{C}_5^A(Q^2) = -C_5^A(0) \left(1 + \frac{Q^2}{M_A^2}\right)^{-2}$$

$$\tilde{C}_4^A(Q^2) = -\frac{\tilde{C}_5^A(Q^2)}{4}, \quad \tilde{C}_3^A(Q^2) = 0 \leftarrow \text{we adopt the Adler model}$$

Adler model: S. L. Adler, Annals Phys 50(1968), 189.

$\Delta(1232)$ Pole Terms – Form Factors

- \tilde{C}_i^V — NC vector form factors
- C_i^V — EM transition form factors
- \tilde{C}_i^A — NC axial form factors

We assume a **standard dipole form** for the axial NC form factors

$$\tilde{C}_5^A(Q^2) = -C_5^A(0) \left(1 + \frac{Q^2}{M_A^2}\right)^{-2}$$

$$\tilde{C}_4^A(Q^2) = -\frac{\tilde{C}_5^A(Q^2)}{4}, \quad \tilde{C}_3^A(Q^2) = 0 \leftarrow \text{we adopt the Adler model}$$

Adler model: S. L. Adler, Annals Phys 50(1968), 189.

The cross section of $\text{NC}\gamma$ strongly depends on $C_5^A(q^2)$.

$\Delta(1232)$ Pole Terms – Form Factors

- \tilde{C}_i^V — NC vector form factors
- C_i^V — EM transition form factors
- \tilde{C}_i^A — NC axial form factors

The axial coupling $C_5^A(0)$ can be expressed in terms of f^*/m_π extracted from the $\Delta \rightarrow \pi N$ decay width through the **off diagonal Goldberger-Treiman relation**

$$C_5^A(0) \approx -\sqrt{\frac{2}{3}} \frac{f^*}{m_\pi} f_\pi.$$

$\Delta(1232)$ Pole Terms – Form Factors

- \tilde{C}_i^V — NC vector form factors
- C_i^V — EM transition form factors
- \tilde{C}_i^A — NC axial form factors

The axial coupling $C_5^A(0)$ can be expressed in terms of f^*/m_π extracted from the $\Delta \rightarrow \pi N$ decay width through the **off diagonal Goldberger-Treiman relation**

$$C_5^A(0) \approx -\sqrt{\frac{2}{3}} \frac{f^*}{m_\pi} f_\pi.$$

- $C_5^A(0) = 1.0 \pm 0.11$ and $M_A = 0.93$ GeV, constrained from the ν -induced π production ($\nu_\mu p \rightarrow \mu^- p \pi^+$) ANL and BNL bubble chamber data. E. Hernandez, et al., PRD 81(2010), 085046

$\Delta(1232)$ Pole Terms – Form Factors

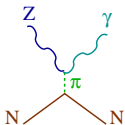
- \tilde{C}_i^V — NC vector form factors
- C_i^V — EM transition form factors
- \tilde{C}_i^A — NC axial form factors

The axial coupling $C_5^A(0)$ can be expressed in terms of f^*/m_π extracted from the $\Delta \rightarrow \pi N$ decay width through the **off diagonal Goldberger-Treiman relation**

$$C_5^A(0) \approx -\sqrt{\frac{2}{3}} \frac{f^*}{m_\pi} f_\pi.$$

- $C_5^A(0) = 1.0 \pm 0.11$ and $M_A = 0.93$ GeV, constrained from the ν -induced π production ($\nu_\mu p \rightarrow \mu^- p \pi^+$) ANL and BNL bubble chamber data. E. Hernandez, et al., PRD 81(2010), 085046
- The uncertainty of our model mainly comes from the N- Δ axial coupling $C_5^A(0)$.

t -channel π Exchange Term



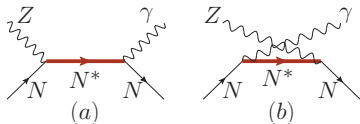
The t -channel pion exchange contribution arises from the anomalous $(\pi^0\gamma Z^0)$ Lagrangian.

$$\Gamma^{\mu\alpha} = -iC_{p,n} \frac{g_A}{4\pi^2 f_\pi^2} \left(\frac{1}{2} - 2\sin^2\theta_W \right) \epsilon^{\sigma\delta\mu\alpha} q_{\gamma\sigma} q_{\delta}(\not{p}' - \not{p})\gamma_5 D_\pi(p' - p),$$

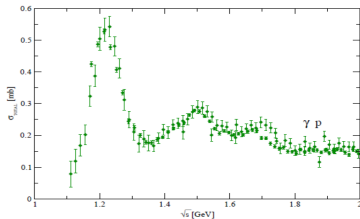
where,

$$C_{p,n} = \pm 1$$
$$D_\pi(p) = \frac{1}{p^2 - m_\pi^2} \leftarrow \pi \text{ propagator}$$

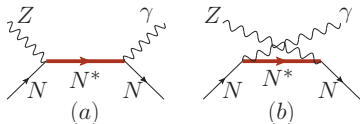
N^* Pole Term [$N(1440)$, $N(1520)$ $N(1535)$]



In order to extend the validity of the model to higher energies, we have considered three isospin 1/2 baryon resonances P_{11} $N(1440)$, D_{13} $N(1520)$ and S_{11} $N(1535)$ from the second resonance region.

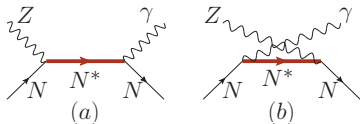


N^* Pole Term [$N(1440)$, $N(1520)$ $N(1535)$]



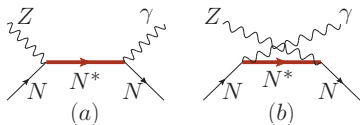
- The hadronic matrix elements of $N(1440)$, $N(1535)$ are similar to that of nucleon pole terms.

N^* Pole Term [$N(1440)$, $N(1520)$ $N(1535)$]



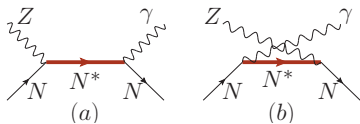
- The hadronic matrix elements of $N(1440)$, $N(1535)$ are similar to that of nucleon pole terms.
- The hadronic matrix element of $N(1520)$ is similar to that of $\Delta(1232)$ pole terms.

N^* Pole Term [$N(1440)$, $N(1520)$ $N(1535)$]



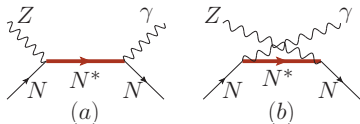
- The hadronic matrix elements of $N(1440)$, $N(1535)$ are similar to that of nucleon pole terms.
- The hadronic matrix element of $N(1520)$ is similar to that of $\Delta(1232)$ pole terms.
- $N - N^*$ vector form factors can be obtained from helicity amplitudes.

N^* Pole Term [$N(1440)$, $N(1520)$ $N(1535)$]



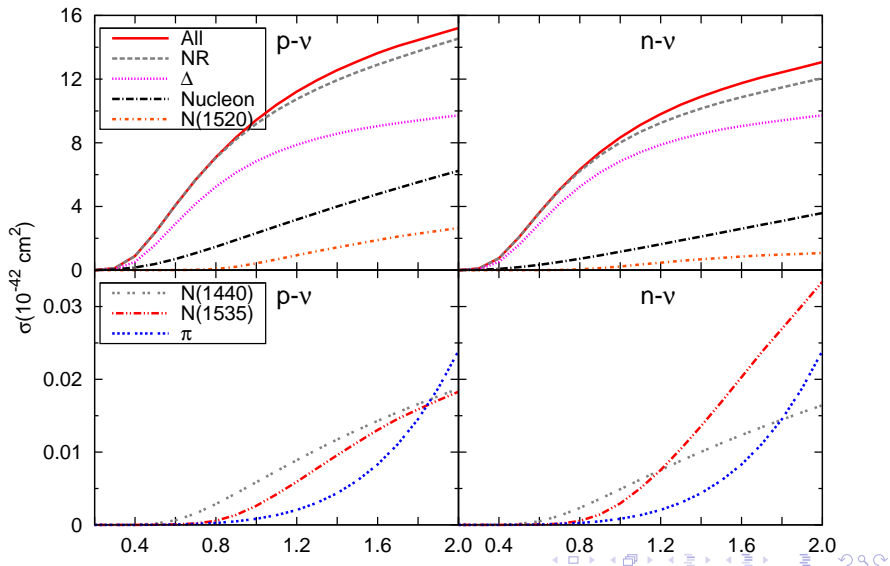
- The hadronic matrix elements of $N(1440)$, $N(1535)$ are similar to that of nucleon pole terms.
- The hadronic matrix element of $N(1520)$ is similar to that of $\Delta(1232)$ pole terms.
- $N - N^*$ vector form factors can be obtained from helicity amplitudes.
- The axial couplings are obtained by the off diagonal Goldberger-Treiman relations.

N^* Pole Term [$N(1440)$, $N(1520)$ $N(1535)$]

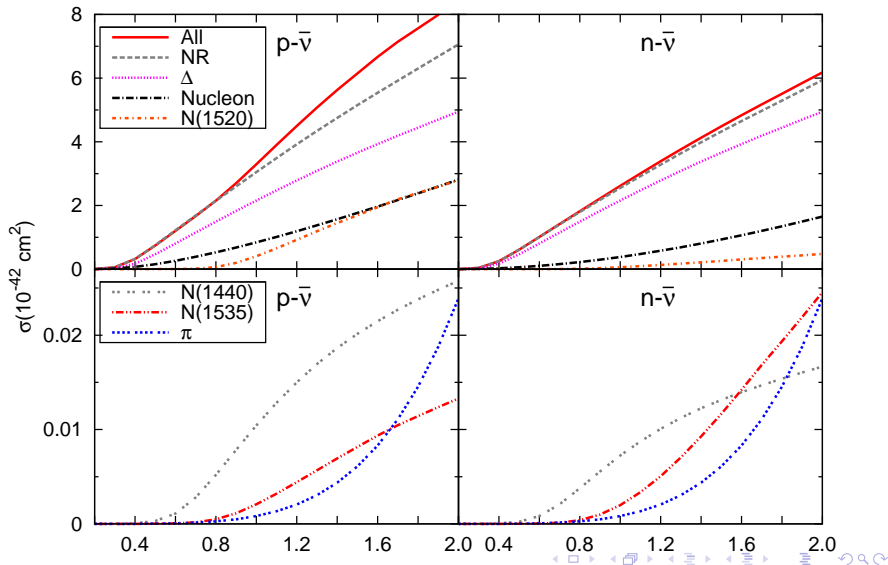


- The hadronic matrix elements of $N(1440)$, $N(1535)$ are similar to that of nucleon pole terms.
- The hadronic matrix element of $N(1520)$ is similar to that of $\Delta(1232)$ pole terms.
- $N - N^*$ vector form factors can be obtained from helicity amplitudes.
- The axial couplings are obtained by the off diagonal Goldberger-Treiman relations.
- We assume a standard dipole form for the axial form factors, and use a natural value for the axial mass $M_A^* = 1.0$ GeV.

NC γ Cross Section on Nucleon for Neutrino



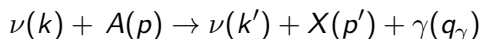
NC γ Cross Section on Nucleon for Antineutrino



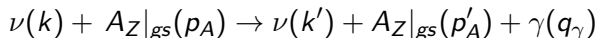
Theoretical model – Incoherent $\text{NC}\gamma$ on nuclei

NC γ on Nuclei

It consists of the incoherent and coherent reactions.



For the **incoherent reaction**, the final nucleus is **either broken or left in some excited state**.



For the **coherent reaction**, the final nucleus is **left in its ground state**.

Incoherent Reaction

The differential cross section for the incoherent reaction is,

$$d\sigma^A = 2 \int d^3\vec{r} \int \frac{d^3\vec{p}}{(2\pi)^3} n_N(\vec{p}, \vec{r}) [1 - n_N(\vec{p}', \vec{r})] d\sigma^N,$$

Incoherent Reaction

The differential cross section for the incoherent reaction is,

$$d\sigma^A = 2 \int d^3\vec{r} \int \frac{d^3\vec{p}}{(2\pi)^3} n_N(\vec{p}, \vec{r}) [1 - n_N(\vec{p}', \vec{r})] d\sigma^N,$$

- Fermi motion: $k_F(\vec{r}) = [3\pi^2 \rho(\vec{r})]^{1/3}$

We adopt the relativistic **local Fermi gas approximation**. The target nucleon moves in a local Fermi sea of momentum k_F defined as a function of the local density of protons and neutrons, independently.

Incoherent Reaction

The differential cross section for the incoherent reaction is,

$$d\sigma^A = 2 \int d^3\vec{r} \int \frac{d^3\vec{p}}{(2\pi)^3} n_N(\vec{p}, \vec{r}) [1 - n_N(\vec{p}', \vec{r})] d\sigma^N,$$

- Fermi motion: $k_F(\vec{r}) = [3\pi^2 \rho(\vec{r})]^{1/3}$
- Pauli blocking: $1 - n(\vec{r}, \vec{p})$

Final nucleons are not allowed to take occupied states.

Incoherent Reaction

The differential cross section for the incoherent reaction is,

$$d\sigma^A = 2 \int d^3\vec{r} \int \frac{d^3\vec{p}}{(2\pi)^3} n_N(\vec{p}, \vec{r}) [1 - n_N(\vec{p}', \vec{r})] d\sigma^N,$$

- Fermi motion: $k_F(\vec{r}) = [3\pi^2 \rho(\vec{r})]^{1/3}$
- Pauli blocking: $1 - n(\vec{r}, \vec{p})$
- In-medium modification of the $\Delta(1232)$ properties

The Δ resonance acquires a selfenergy because of several effects such as Pauli blocking of the final nucleon and absorption processes: $\Delta N \rightarrow NN$, $\Delta N \rightarrow NN\pi$ or $\Delta NN \rightarrow NNN$. E. Oset and L. Salcedo, NPA 468(1987), 631

Incoherent Reaction

The differential cross section for the incoherent reaction is,

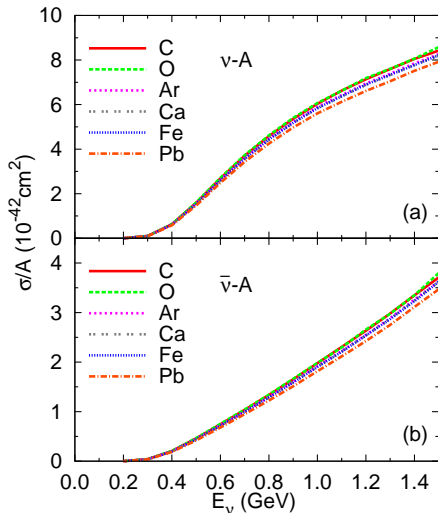
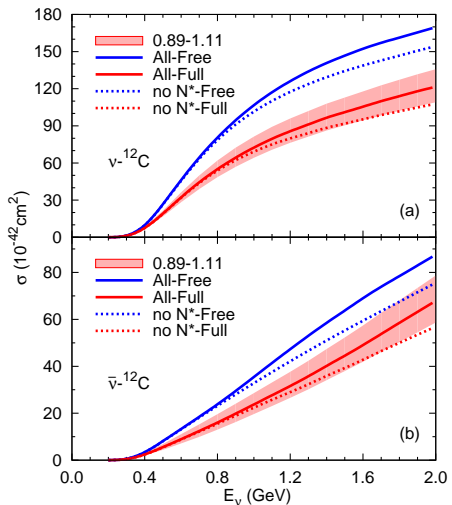
$$d\sigma^A = 2 \int d^3\vec{r} \int \frac{d^3\vec{p}}{(2\pi)^3} n_N(\vec{p}, \vec{r}) [1 - n_N(\vec{p}', \vec{r})] d\sigma^N,$$

- Fermi motion: $k_F(\vec{r}) = [3\pi^2\rho(\vec{r})]^{1/3}$
- Pauli blocking: $1 - n(\vec{r}, \vec{p})$
- In-medium modification of the $\Delta(1232)$ properties

$$D_\Delta(p) = \frac{1}{p^2 - M_\Delta^2 + iM_\Delta\Gamma_\Delta(p^2)},$$

- $\Gamma_\Delta/2 \rightarrow \Gamma_\Delta^{\text{Pauli}}/2 - \text{Im}\Sigma_\Delta(\rho)$
- $\Gamma_\Delta^{\text{Pauli}}$ — free width of $\Delta \rightarrow N\pi$ modified by Pauli blocking
- $\text{Im}\Sigma_\Delta(\rho)$, includes many body processes:
 $\Delta N \rightarrow NN$, $\Delta N \rightarrow NN$ and $\Delta NN \rightarrow NNN$

Incoherent Reaction



Theoretical model – Coherent $\text{NC}\gamma$ on nuclei

Coherent Reaction

The amplitude is given by,

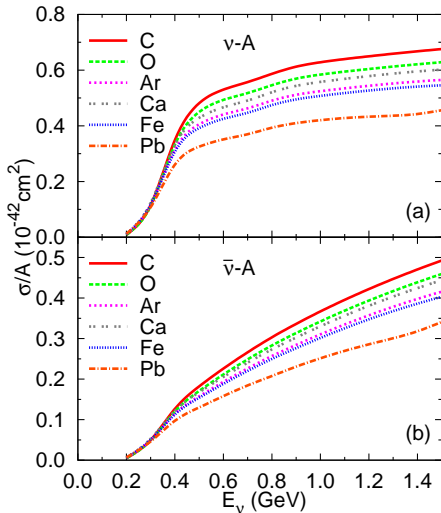
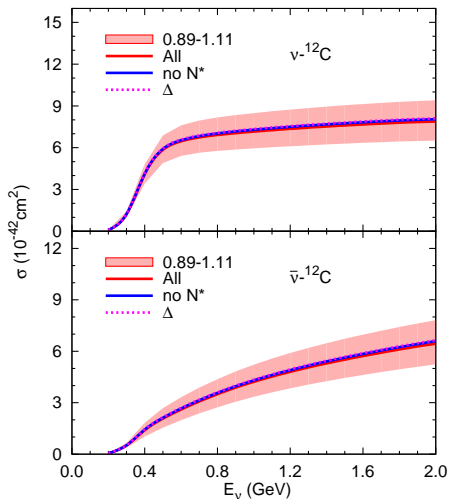
$$\mathcal{M}_r = \frac{G_F}{\sqrt{2}} I_\alpha J_{coh(r)}^\alpha,$$

the hadronic current $J_{coh(r)}^\alpha$ is given by,

$$J_{coh(r)}^\alpha = ie\epsilon_\mu^{*(r)} \int d^3\vec{r} e^{i(\vec{q}-\vec{q}_\gamma)\cdot\vec{r}} (\rho_p(r)\Gamma_p^{\mu\alpha} + \rho_n(r)\Gamma_n^{\mu\alpha})$$

- After the coherent sum over of all nucleons, one obtains the nucleon densities. The coherent process is sensitive to the Fourier transform of the nuclear density.
- nuclear correction: $\Gamma_\Delta/2 \rightarrow \Gamma_\Delta^{\text{Pauli}}/2 - \text{Im}\Sigma_\Delta(\rho)$

Coherent Reaction



NC γ events at MiniBooNE

(PLB 740(2015),16)

CCQE Reconstructed (Anti)Neutrino Energy

- As a source of irreducible background to the electron CCQE events from $\nu_\mu \rightarrow \nu_e$ ($\bar{\nu}_\mu \rightarrow \bar{\nu}_e$) oscillations, it is important to predict the event distribution as a function of E_ν^{QE} .
- In the MiniBooNE study, E_ν^{QE} is determined from the energy and angle of the outgoing electron, assuming that it was originated in a $\nu n \rightarrow e^- p$ ($\bar{\nu} p \rightarrow e^+ n$) interaction on a bound neutron (proton) at rest

$$E_\nu^{\text{QE}} = \frac{2(M_N - E_B)E_e - [E_B^2 - 2M_N E_B + m_e^2 + \Delta M^2]}{2[(M_N - E_B) - E_e(1 - \cos\theta_e)]}.$$

- When photons from NC γ events are misidentified as electrons, E_ν^{QE} is misreconstructed according to the above equation, with E_γ and θ_γ replacing the energy and angle of the outgoing electron E' and θ' . The binding energy $E_B = 34$ MeV.

The Events

NC γ events at the MiniBooNE detector is given by,

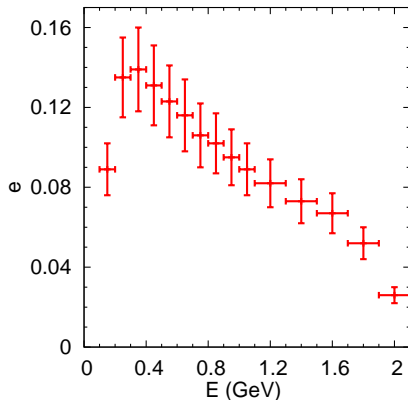
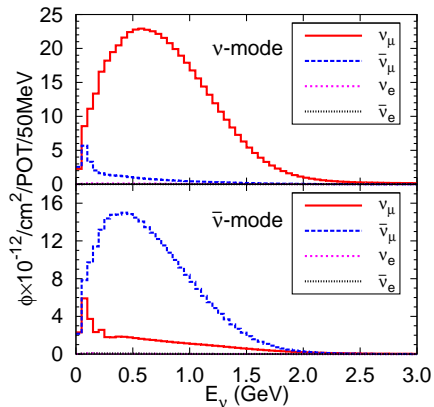
$$\frac{dN}{dE_\gamma d \cos \theta_\gamma} = \varepsilon(E_\gamma) \sum_{l=\nu_\mu, \bar{\nu}_\mu} N_{\text{POT}}^{(l)} \times \sum_{t=p, {}^{12}\text{C}} N_t \int dE_\nu \phi_l(E_\nu) \frac{d\sigma_{lt}(E_\nu)}{dE_\gamma d \cos \theta_\gamma}.$$

- $d\sigma_{lt}(E_\nu)/(dE_\gamma d \cos \theta_\gamma)$: cross section for NC γ on proton, incoherent and coherent reaction on Carbon
- $N_{\text{POT}}^{(l)}$: the total number of protons on target (POT)
 $N_{\text{POT}}^\nu = 6.46 \times 10^{20}$ and $N_{\text{POT}}^{\bar{\nu}} = 11.27 \times 10^{20}$
- N_t : the number of protons/carbon nuclei in the target (806 tons CH₂)
- $\varepsilon(E_\gamma)$: energy dependent detection efficiency
- $\phi_l(E_\nu)$: neutrino/antineutrino fluxes

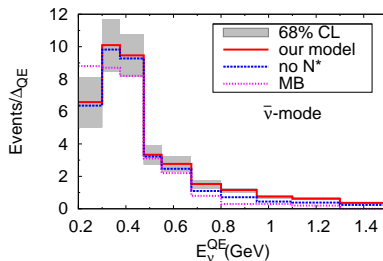
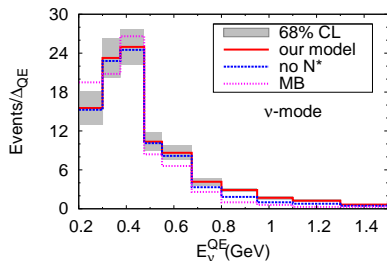
A. Aguilar-Arevalo et al., PRL 102(2009), 101802; 110(2013), 161801

http://www-boone.fnal.gov/for_physicists/data_release/nue_nuebar_2012

Beam Flux and Detection Efficiency at MiniBooNE



Comparison to The MB Estimate

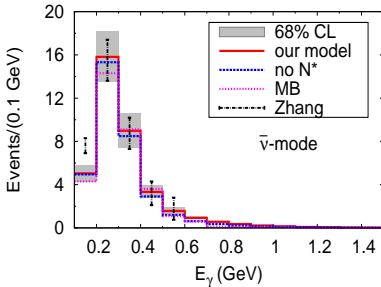
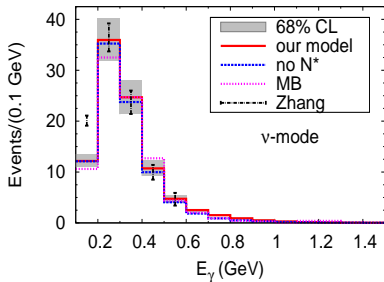


- The comparison shows a good agreement, the shapes are similar and the peak positions coincide.
- The largest discrepancy is observed in the lowest energy bin.
- The inclusion of the N^* increases the difference, which might be due to the fact that the resonances contributions at MB is calculated with the phenomenologically outdated model of Rein and Sehgal.

D. Rein and L. Sehgal, *Annals Phys.* 133 (1981), 79,

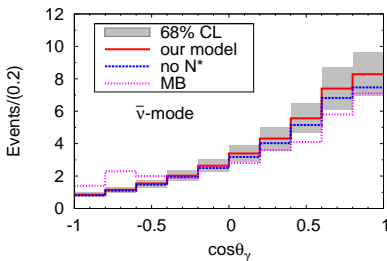
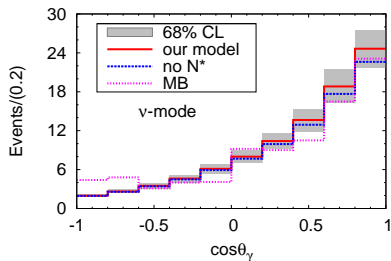
L. Alvarez-Ruso, Y. Hayato, and J. Nieves, *New J.Phys.*, 16(2014), 075015.

E_γ Distribution of The Photon Events



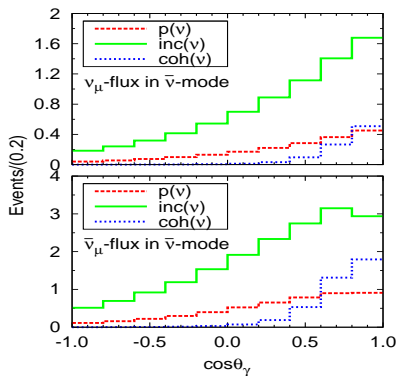
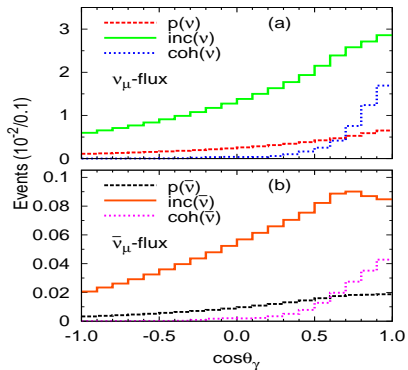
The agreement of the full model with the MiniBooNE estimate is very good for this observable, even at the lowest photon-energy bin,

$\cos\theta_\gamma$ Distribution of The Photon Events



We predict more forward peaked distributions than MiniBooNE does. This is not surprising as we have sizable coherent contributions, not considered in the MiniBooNE estimate.

$\cos\theta_\gamma$ Distribution of The Photon Events



Conclusion

- With our microscopic model, we have calculated event distributions (E_ν^{QE} , E_γ and $\cos\theta_\gamma$) from NC γ to the electron-like irreducible background at the MiniBooNE experiment.

Conclusion

- With our microscopic model, we have calculated event distributions (E_ν^{QE} , E_γ and $\cos\theta_\gamma$) from NC γ to the electron-like irreducible background at the MiniBooNE experiment.
- The largest contribution arises from the incoherent reaction on ^{12}C , and the interactions on the two protons and coherent scattering on ^{12}C produce sizable, and similar in magnitude contributions.

Conclusion

- With our microscopic model, we have calculated event distributions (E_ν^{QE} , E_γ and $\cos\theta_\gamma$) from NC γ to the electron-like irreducible background at the MiniBooNE experiment.
- The largest contribution arises from the incoherent reaction on ^{12}C , and the interactions on the two protons and coherent scattering on ^{12}C produce sizable, and similar in magnitude contributions.
- Our results are in good agreement with MiniBooNE in situ estimate, and we conclude that photon emission processes from single-nucleon currents cannot explain the excess of the signal-like events observed at MiniBooNE.

NC γ events at T2K

(arXiv:1507.02446 [hep-ph])

T2K Detector

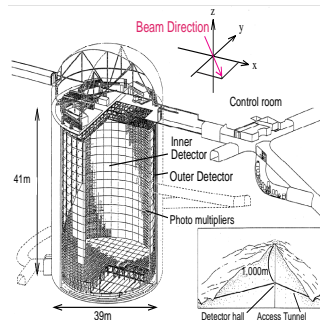
- The neutrino mixing angle θ_{13} has been precisely measured from $\bar{\nu}_e$ disappearance in nuclear reactor neutrino experiments Daya Bay, RENO, DOUBLE-CHOOZ). [PRL112, 061801 (2014), PRL108, 191802 (2012), PRL108, 131801 (2012)]
- The tension between reactor data and T2K favors a $\delta_{CP} = -2/\pi$ at 90% C.L., although the picture is still far from clear because the MINOS combined ν_μ disappearance and ν_e appearance prefers a $\delta_{CP} = 2/\pi$. [PRL112, 061802 (2014), PRL112, 191801 (2014)]
- Further progress in this direction requires a better control over systematic errors and, in particular, of irreducible backgrounds.
- Super-Kamiokande (SK), the far detector of the T2K experiment, is a water Cherenkov detector and incapable of discriminating the diffuse rings of e^\pm originated in charged current interactions by electron neutrinos from those created by photons.

T2K Detector

- Super-Kamiokande (SK), the far detector of T2K experiment is a water Cherenkov detector.

Target: H_2O , Mass: 22.5 ktons

- POT: 6.57×10^{20} (ν mode)
- Flux: SK250 $0.1 < E_\nu < 3 \text{ GeV}$

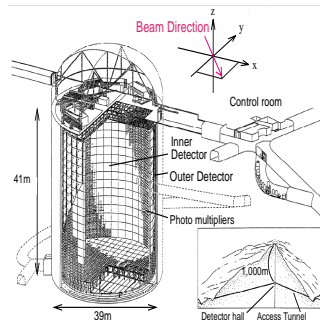


T2K Detector

- Super-Kamiokande (SK), the far detector of T2K experiment is a water Cherenkov detector.

Target: H_2O , Mass: 22.5 ktons

- POT: 6.57×10^{20} (ν mode)
- Flux: SK250 $0.1 < E_\nu < 3 \text{ GeV}$



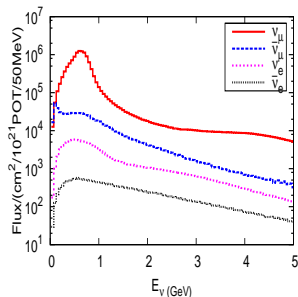
We have applied our microscopic model for the $\text{NC}\gamma$ reaction to predict the number of $\text{NC}\gamma$ events at the SK detector.

T2K Detector

- Super-Kamiokande (SK), the far detector of T2K experiment is a water Cherenkov detector.

Target: H_2O , Mass: 22.5 ktons

- POT: 6.57×10^{20} (ν mode)
- Flux: SK250 $0.1 < E_\nu < 3 \text{ GeV}$



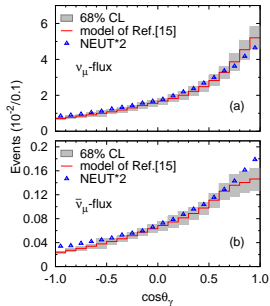
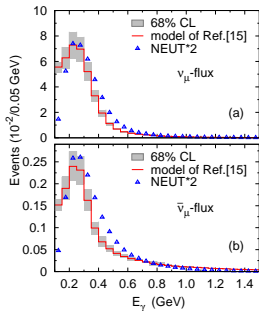
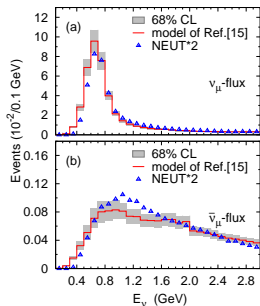
We have applied our microscopic model for the $\text{NC}\gamma$ reaction to predict the number of $\text{NC}\gamma$ events at the SK detector.

Comparison With T2K Estimate of NEUT Generator (V5.1.2.4)

$$\mathcal{N}_{\text{total}} = 0.427 \pm 0.050 \quad \text{VS} \quad \mathcal{N}_{\text{NEUT}} = 0.217$$

Comparison With T2K Estimate of NEUT Generator (V5.1.2.4)

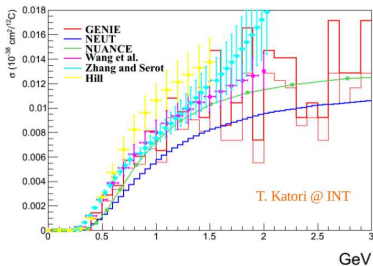
$$\mathcal{N}_{\text{total}} = 0.427 \pm 0.050 \quad \text{VS} \quad \mathcal{N}_{\text{NEUT}} = 0.217$$



Comparison With T2K Estimate of NEUT Generator (V5.1.2.4)

- The cross section for ν -induced coherent NC γ reaction on ^{12}C

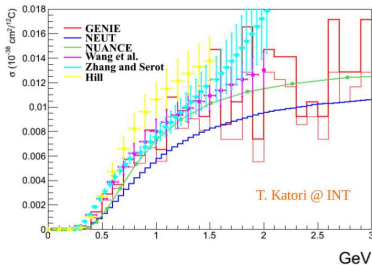
T. Katori, J. Conrad, Adv.High Energy Phys. 2015 (2015) 362971



Comparison With T2K Estimate of NEUT Generator (V5.1.2.4)

- The cross section for ν -induced coherent NC γ reaction on ^{12}C

T. Katori, J. Conrad, Adv.High Energy Phys. 2015 (2015) 362971



- The disagreement is likely due to the discrepancy in the size of the integrated cross sections in the two models.

Comparison With T2K Estimate of NEUT Generator

Our prediction is **twice larger** than the T2K estimate from the NEUT Monte Carlo generator.

No significant difference in the shape of E_ν , E_γ and $E_{\cos\theta_\gamma}$ distributions.

The T2K near detector ND280 may be able to constrain the NEUT prediction by selecting γ candidate events in the future.

To me, this is one of the largest experimental holes we have on T2K— we have no real data constraint on this channel so it's very critical to get theoretical input.—Kendall Mahn

Thank you!